ICECUBE NON-DETECTION OF GRBS: CONSTRAINTS ON THE FIREBALL PROPERTIES

Hao-Ning He[1,2,3], Ruo-Yu Liu[1,2], Xiang-Yu Wang[1,2], Shigehiro Nagataki[3], Kohta Murase[4], Zi-Gao Dai[1,2]

Draft version March 2, 2013

ABSTRACT

The increasingly deep limit on the neutrino emission from gamma-ray bursts (GRBs) with IceCube observations has reached the level that could put useful constraints on the fireball properties. We first present a revised analytic calculation of the neutrino flux, which predicts a flux an order of magnitude lower than that obtained by the IceCube collaboration. For benchmark model parameters (e.g. the bulk Lorentz factor is $\Gamma = 10^{2.5}$, the observed variability time for long GRBs is $t_{\rm v}^{\rm ob} = 0.01$s and the ratio between the energy in accelerated protons and in radiation is $\eta_p = 10$ for every burst) in the standard internal shock scenario, the predicted neutrino flux from 215 bursts during the period of the 40-string and 59-string configurations is found to be a factor of ~ 3 below the IceCube sensitivity. However, if we accept the recently found inherent relation between the bulk Lorentz factor and burst energy, the expected neutrino flux increases significantly and the spectral peak shifts to lower energy. In this case, the non-detection then implies that the baryon loading ratio should be $\eta_p \lesssim 10$ if the variability time of long GRBs is fixed to $t_{\rm v}^{\rm ob} = 0.01$s. Instead, if we relax the standard internal shock scenario but keep to assume $\eta_p = 10$, the non-detection constrains the dissipation radius to be $R \gtrsim 4 \times 10^{12}$cm assuming the same dissipation radius for every burst and benchmark parameters for fireballs. We also calculate the diffuse neutrino flux from GRBs for different luminosity functions existing in the literature. The expected flux exceeds the current IceCube limit for some luminosity functions, and thus the non-detection constrains $\eta_p \lesssim 10$ in such cases when the variability time of long GRBs is fixed to $t_{\rm v}^{\rm ob} = 0.01$s.

Subject headings: gamma-ray bursts—neutrino

1. INTRODUCTION

GRBs have been proposed as one of the potential sources for ultra-high energy cosmic rays (UHECRs) with energy up to $> 10^{20}$eV (e.g. Waxman 1995; Vietri 1995; Waxman & Bahcall 2000; Dai & Lu 2001; Dermer 2002; Murase et al. 2006), given the hypothesis that the fireball composition is proton-dominated and the protons get accelerated in the dissipative fireballs. Interactions of protons with fireball photons will produce a burst of neutrinos with energies of $\sim$PeV (e.g. Waxman &Bahcall 1997; Guetta et al. 2004; Dermer & Atoyan 2006), so detection of such neutrinos would prove the presence of cosmic ray protons in the fireball. Despite that large progresses in the studies of GRBs and their afterglow have been made recently, the composition of the jet, whether it is proton-electron dominated or Poynting-flux dominated, is largely unknown. Both baryon-dominated fireball shock model (e.g. Rees & Mészáros 1994; Paczyński & Xu 1994) and magnetic dissipation model (e.g. Narayan & Kumar 2009; Zhang & Yan 2010) have been proposed for the central engine of GRBs. In the magnetically dominated outflow model for GRBs, the non-thermal proton energy fraction may

be low (but see Giannios 2010), while in the baryon-dominated outflow model, it is natural to expect proton acceleration via shock dissipation of the kinetic energy. Since the flux of neutrinos depends on the energy fraction of protons in the fireball for a given burst energy, the flux or limit of the neutrino emission could constrain the proton energy fraction and in principal provide a useful probe of the jet composition. The proton energy fraction is also crucial to know whether GRBs could provide sufficient flux for UHECRs.

The Kilometer-scale IceCube detector is the most sensitive neutrino telescope in operation, although no positive neutrino signal has been detected so far (Abbasi et al. 2010, 2011a; The IceCube collaboration 2011). The IceCube operations with the 22, 40 and 59 strings configurations all yield negative results, which have put more and more stringent constraints on neutrino emission from GRBs. The analysis were performed for both point source search from individual GRBs and diffuse emission from aggregated GRBs (Abbasi et al. 2011b). According to the IceCube collaboration, with 40-string configuration operation between 2008 and 2009, IceCube reaches a sensitivity at the level of the expect flux from GRBs and the combined upper limit of IceCube 40-string and IceCube 59-string analysis is 0.22 times the expected flux (Abbasi et al. 2011a). Based on this, the IceCube collaboration argued that the UHECR-GRB connection is challenged (Abbasi et al. 2011a).

The calculation by the IceCube collaboration (ICC hereafter) is based on the formula in the appendix of the paper Abbasi et al. (2010) and benchmark parameters for the internal shock model of GRBs. However, as also pointed out by Li (2011) and Hümmer et al. (2011), we

[1] School of Astronomy and Space Science, Nanjing University, Nanjing, 210093, China; haoninghe@nju.edu.cn, ryliu@nju.edu.cn, xywang@nju.edu.cn
[2] Key laboratory of Modern Astronomy and Astrophysics (Nanjing University), Ministry of Education, Nanjing 210093, China
[3] Yukawa Institute for Theoretical Physics, Kyoto University, Oiwakecho, Kitashirakawa, Sakyoku, Kyoto 606-8502, Japan
[4] Department of Physics, Center for Cosmology and AstroParticle Physics, The Ohio State University, Columbus, OH 43210, USA

will show that the normalization procedure used by ICC overestimates the neutrino flux. In calculating the photon number density, ICC also approximates the energy of all photons by the break energy of the photon spectrum, which originates from the assumption in Guetta et al. 2004 (GT2004 hereafter). To get a more accurate estimate of the expected neutrino flux, we first present a refined analytic calculation in § 2.1, revising the above approximations, and perform a numerical calculation in § 2.2 taking into account three main energy loss channels for protons interacting with burst photons. In § 3, we study the effects of non benchmark parameters on the neutrino emission, such as the dissipation radius and the bulk Lorentz factor of the fireball. In § 4, we calculate the accumulative diffuse neutrino emission from GRBs and confront it with the IceCube limit on diffuse neutrinos. At the end, we give our conclusions and discussions.

2. GRB NEUTRINO SPECTRA

Based on the assumption that protons and electrons are accelerated in the same region of a GRB, protons interact with photons emitted by electron synchrotron emission or inverse-Compton emission predominantly produce the charged and neutral pions. The charged pion subsequently decays to produce 4 final state leptons, via the processes $\pi^{\pm} \rightarrow \nu_{\mu}(\bar{\nu}_{\mu})\mu^{\pm} \rightarrow \nu_{\mu}(\bar{\nu}_{\mu})e^{+}(e^{-})\nu_{e}(\bar{\nu}_{e})\bar{\nu}_{\mu}(\nu_{\mu})$, which approximately share the pion energy equally. Denoting $\Re$ as the ratio between the charged pion number to the total pion number, the fraction of the proton energy lost into each lepton is $\frac{\Re}{4}f_{p\gamma}$, where $f_{p\gamma}$ is the fraction of the protons energy lost into pions. For the proton with energy of $\epsilon_p = \gamma_p m_p c^2$, the photomeson interaction timescale can be calculated by (Waxman & Bahcall 1997)

$$
\begin{aligned}
t_{p\gamma}^{-1}(\epsilon_p) &= \frac{1}{\epsilon_p}\frac{d\epsilon_p}{dt} \\
&= \frac{c}{2\gamma_p^2}\int_{\tilde{\epsilon}_{\gamma,\text{th}}}^{\infty}d\tilde{\epsilon}_{\gamma}\sigma_{p\gamma}(\tilde{\epsilon}_{\gamma})\xi(\tilde{\epsilon}_{\gamma})\tilde{\epsilon}_{\gamma}\int_{\tilde{\epsilon}_{\gamma}/2\gamma_p}^{\infty}dx x^{-2}\frac{dn_{\gamma}}{dx},
\end{aligned}
\tag{1}
$$

where $\sigma_{p\gamma}(\tilde{\epsilon}_{\gamma})$ is the cross section of photomeson interaction for a photon with energy $\tilde{\epsilon}_{\gamma}$ in the proton-rest frame, $\xi(\tilde{\epsilon}_{\gamma})$ is the inelasticity, $\tilde{\epsilon}_{\gamma,\text{th}}$ is the threshold of photon energy and $\frac{dn_{\gamma}}{d\epsilon_{\gamma}}$ is the GRB photon spectrum in fluid-rest frame (Waxman & Bahcall 1997). The fraction of protons energy loss into pions is

$$
f_{p\gamma} = 1 - \exp(-t_{\text{dyn}}/t_{p\gamma}),
\tag{2}
$$

where $t_{\text{dyn}} = R/(\Gamma c)$ is the dynamic timescale. Just for simplicity, we use t_{dyn} as the interaction time. Generally speaking, proton cooling timescales can be shorter than the dynamical timescale (see Murase & Nagataki 2006a,b, for details), but we do not consider such complicated effects for the purpose of testing the standard model suggested by Waxman & Bahcall (1997) (Hummer et al. 2012).

Approximating that neutrinos produced via photomeson interaction by proton with energy ϵ_p have constant energy, the spectrum of neutrinos from the decay of secondary particles can be obtained by, without considering the oscillation,

$$
\epsilon_{\ell}\frac{dn_{\ell}}{d\epsilon_{\ell}}\text{d}\epsilon_{\ell} = \frac{\Re(\epsilon_p)}{4}f_{p\gamma}(\epsilon_p)\theta_{\ell}(\epsilon_p)\epsilon_p\frac{dn_p}{d\epsilon_p}\text{d}\epsilon_p,
\tag{3}
$$

where $\frac{dn_p}{d\epsilon_p}$ is the spectrum of protons and $\Re$ is the ratio between the charged pion number to the total pion number as defined above equation (1). The subscript ℓ represents different flavors of neutrinos, i.e., $\ell = \nu_{\mu}, \bar{\nu}_{\mu}, \nu_{e}$ for muon neutrinos ν_{μ} produced via the decay of pions, antimuon neutrinos $\bar{\nu}_{\mu}$ and electron neutrinos ν_{e} produced via the decay of muons, respectively. If the cooling timescale of pions or muons is smaller than their lifetime, pions or muons have the probability to cool down before decay. Then the neutrino flux will be suppressed by a factor of $\zeta_{\pi} = 1 - \exp\left(-t_{\pi,\text{syn}}/\tau_{\pi}\right)$, where $t_{\pi,\text{syn}} = 3.3\times 10^{-3}\text{s}L_{\gamma,52}^{-1}\Gamma_{2.5}^2 R_{14}^2\epsilon_{\pi,\text{EeV}}^{-1}$ is the synchrotron cooling timescale, and $\tau_{\pi} = 2.6\times 10^{-8}\text{s}\gamma_{\pi} = 186\text{s}\epsilon_{\pi,\text{EeV}}$ is the lifetime of pions, whose energy is $\epsilon_{\pi} = 0.2\epsilon_{\text{p}}$. Here we assume the fraction of electron energy and magnetic field energy are same, i.e., $\epsilon_e = \epsilon_B$. Similarly, the suppression due to muon cooling is $\zeta_{\mu} = 1-\exp\left(-t_{\mu,\text{syn}}/\tau_{\mu}\right)$, where $t_{\mu,\text{syn}} = 1.1\times 10^{-3}\text{s}L_{\gamma,52}^{-1}\Gamma_{2.5}^2 R_{14}^2\epsilon_{\mu,\text{EeV}}^{-1}$ and $\tau_{\mu} = 2.1\times 10^4\text{s}\epsilon_{\mu,\text{EeV}}$ with the muon energy $\epsilon_{\mu} = 0.15\epsilon_{\text{p}}$. The suppression factor $\theta_{\ell}(\epsilon_p)$ is a combination of $\zeta_{\pi}(\epsilon_p)$ and $\zeta_{\mu}(\epsilon_p)$, i.e., $\theta_{\nu_{\mu}}(\epsilon_p) = \zeta_{\pi}(\epsilon_p)$ and $\theta_{\bar{\nu}_{\mu}(\nu_e)}(\epsilon_p) = \zeta_{\pi}(\epsilon_p)\zeta_{\mu}(\epsilon_p)$.

Considering the neutrino oscillation effect, the spectrum of muon neutrinos (including antimuon neutrinos) detected on Earth is approximated as (Nagataki et al. 2003; Particle Data Group 2004; Kashti & Waxman 2005; Murase 2007; Li 2011)

$$
\frac{dn_{\nu}}{d\epsilon_{\nu}} = 0.2\frac{dn_{\nu_e}}{d\epsilon_{\nu_e}} + 0.4\frac{dn_{\nu_{\mu}}}{d\epsilon_{\nu_{\mu}}} + 0.4\frac{dn_{\bar{\nu}_{\mu}}}{d\epsilon_{\bar{\nu}_{\mu}}},
\tag{4}
$$

where ν_{μ} are produced via the decay of secondary pions, and ν_e and $\bar{\nu}_{\mu}$ are produced via the decay of secondary muons. Therefore, by inserting equation (3) into equation (4), one can calculate the total spectrum of muon (including antimuon) neutrinos detected on Earth numerically via the following equation:

$$
\epsilon_{\nu}\frac{dn_{\nu}}{d\epsilon_{\nu}}\text{d}\epsilon_{\nu} = \frac{\Re(\epsilon_p)}{4}f_{p\gamma}(\epsilon_p)\theta_{\nu}(\epsilon_p)\epsilon_p\frac{dn_p}{d\epsilon_p}\text{d}\epsilon_p,
\tag{5}
$$

with the factor $\theta_{\nu}(\epsilon_p) = 0.4\zeta_{\pi}(\epsilon_p) + 0.6\zeta_{\pi}(\epsilon_p)\zeta_{\mu}(\epsilon_p)$ accounting for the neutrino oscillation and the cooling of secondary particles.

The GRB photon distribution can be described by

$$
\frac{dn_{\gamma}}{d\epsilon_{\gamma}} = A_{\gamma}\left(\frac{\epsilon_{\gamma}}{\epsilon_{\gamma\text{b}}}\right)^{-q}
\tag{6}
$$

where $\epsilon_{\gamma,b}$ is the break energy (in the fluid-rest frame) of the photon spectrum, $q = \alpha$ for $\epsilon_{\gamma} < \epsilon_{\gamma b}$ and $q = \beta$ for $\epsilon_{\gamma} > \epsilon_{\gamma b}$. The normalized coefficient is $A_{\gamma} = U_{\gamma}[\int_{\epsilon_{\gamma,\text{min}}}^{\epsilon_{\gamma,\text{max}}}\epsilon_{\gamma}\left(\frac{\epsilon_{\gamma}}{\epsilon_{\gamma\text{b}}}\right)^{-q}d\epsilon_{\gamma}]^{-1} = \frac{U_{\gamma}}{y_1\epsilon_{\gamma\text{b}}^2}$, where the energy density of photons is $U_{\gamma} = \frac{L_{\gamma}}{4\pi R^2\Gamma^2 c}$, and

$$
y_1 = \frac{1}{\alpha - 2}\left(\frac{\epsilon_{\gamma\text{b}}}{\epsilon_{\gamma,\text{min}}}\right)^{\alpha-2} - \frac{1}{\beta - 2}\left(\frac{\epsilon_{\gamma\text{b}}}{\epsilon_{\gamma,\text{max}}}\right)^{\beta-2} - \frac{1}{\alpha - 2} + \frac{1}{\beta - 2}
\tag{7}
$$

for $\beta \neq 2$, where $\epsilon_{\gamma,\min}$ and $\epsilon_{\gamma,\max}$ are the minimum and maximum energy of the photons. For $\beta = 2$, $y_1 = \left(1 - \left(\frac{\epsilon_{\gamma,\min}}{\epsilon_{\gamma b}}\right)^{-\alpha+2}\right)/(-\alpha+2) + \ln\left(\frac{\epsilon_{\gamma,\max}}{\epsilon_{\gamma b}}\right)$. Hereafter, we adopt assumptions that $\epsilon_{\gamma,\min} = 1$keV and $\epsilon_{\gamma,\max} = 10$MeV as ICC did (Abassi et al. 2010). If we know redshift of bursts, the correction should be properly taken into account in estimating the luminosity.

The proton number per energy interval can be described by $\frac{dn_p}{d\epsilon_p} = N_p \epsilon_p^{-s}$ with s being the power-law index and N_p being the normalized coefficient. The normalized coefficient of the injected proton spectrum can be calculated by $N_p = E_p / \int_{\epsilon_{p,\min}}^{\epsilon_{p,\max}} d\epsilon_p \epsilon_p^{1-s} = E_p / \ln\frac{\epsilon_{p,\max}}{\epsilon_{p,\min}}$ (we set $s = 2$ hereafter, as predicted by the shock acceleration theory) with E_p being the total energy in protons, $\epsilon_{p,\min}$ and $\epsilon_{p,\max}$ being the minimum and maximum energy of accelerated protons, respectively. We introduce a factor η_p, denoting the ratio of the energy in accelerated protons to the radiation energy, then the total proton energy E_p is (Murase & Nagataki 2006a)

$$E_p = \eta_p E_{\mathrm{iso}} \qquad (8)$$

where E_{iso} is the isotropic energy of the burst, which is obtained from the observed fluence F_γ^{ob} in the energy band of 1 keV - 10 MeV and the redshift of the burst. According to Waxman (1995) and Li (2011), for mildly-relativistic GRB internal shocks, we assume the minimum proton energy as $\epsilon_{p,\min}^{\mathrm{ob}} \simeq \Gamma m_p c^2 = 3.0 \times 10^{11} \Gamma_{2.5}/(1+z)$eV [5] , and the maximum proton energy due to synchrotron cooling is $\epsilon_{p,\max}^{\mathrm{ob}} = 4.0 \times 10^{20} \Gamma_{2.5}^{3/2} R_{14}^{1/2} \epsilon_e^{1/4} \epsilon_B^{-1/4} g_1^{-1/2} L_{\gamma,52}^{-1/4}/(1+z)$eV, with $g_1 \gtrsim 1$ being a factor accounting for the uncertainty in the particle acceleration time.

2.1. Analytical Calculation
2.1.1. Neutrino spectrum in the general dissipation scenario

In this subsection, we treat the dissipation radius as a free parameter, since the exact dissipation mechanism of GRBs is not established. There are suggestions that, besides the standard internal shock model, the prompt emission arises from the dissipative photosphere or arises at much larger radii where the magnetic-dominated outflow is dissipated through magnetic dissipation processes, such as reconnection (e.g. Narayan & Kumar 2009, Kumar & Narayan 2009, Zhang & Yan 2010).

For the analytical calculation, we adopt the Δ resonance approximation as in Waxman & Bahcall (1997) and Guetta et al. (2004), where the cross section peaks at the photon energy $\tilde{\epsilon}_\gamma \sim \epsilon_{\mathrm{peak}} = 0.3$GeV in the proton-rest frame. If $t_{\mathrm{dyn}} < t_{p\gamma}$, the conversion fraction is approximated as $f_{p\gamma} \simeq t_{\mathrm{dyn}}/t_{p\gamma} = R/(\Gamma c t_{p\gamma})$. Adopting the Δ resonance approximation (Waxman & Bahcall 1997), the fraction of proton energy converted into pion

---

is

$$f_{p\gamma}(\epsilon_p^{\mathrm{ob}}) \simeq \frac{0.11}{y_1}\left(\frac{2}{\alpha+1}\right)\left(\frac{1}{1+z}\right)\frac{L_{\gamma 52}}{\epsilon_{\gamma b,\mathrm{MeV}}^{\mathrm{ob}}\Gamma_{2.5}^2 R_{14}}$$

$$\times \begin{cases} k_1 \left(\frac{\epsilon_p^{\mathrm{ob}}}{\epsilon_{p,b}^{\mathrm{ob}}}\right)^{\beta-1}, & \epsilon_p^{\mathrm{ob}} \leq \epsilon_{p,b}^{\mathrm{ob}} \\ \left(\frac{\epsilon_p^{\mathrm{ob}}}{\epsilon_{p,b}^{\mathrm{ob}}}\right)^{\alpha-1} + k_p, & \epsilon_p^{\mathrm{ob}} > \epsilon_{p,b}^{\mathrm{ob}} \end{cases} \qquad (9)$$

where

$$\epsilon_{p,b}^{\mathrm{ob}} = \Gamma_p^{\mathrm{ob}} m_p c^2 = \frac{\Gamma^2 \xi_{\mathrm{peak}}}{2(1+z)^2 \epsilon_{\gamma b}^{\mathrm{ob}}}, \qquad (10)$$

$k_1 = \frac{\alpha+1}{\beta+1}$ and $k_p = \frac{\alpha-\beta}{\beta+1}\left(\frac{\epsilon_p^{\mathrm{ob}}}{\epsilon_{p,b}^{\mathrm{ob}}}\right)^{-2}$ [6]. Note that the above approximation is valid when the radius is not too small, i.e., $R > 1.1 \times 10^{13}\left(\frac{1}{y_1}\right)\left(\frac{2}{\alpha+1}\right)\left(\frac{1}{1+z}\right)L_{\gamma,52}\epsilon_{\gamma b,\mathrm{MeV}}^{\mathrm{ob},-1}\Gamma_{2.5}^{-2}$cm.

As $\epsilon_\nu = 0.05\epsilon_p$ for the Δ resonance approximation, from equation (10), we can obtain the break energy of neutrino spectrum corresponding to the photon spectral break

$$\epsilon_{\nu,b}^{\mathrm{ob}} = 7.5 \times 10^5 \mathrm{GeV}(1+z)^{-2}\Gamma_{2.5}^2 \epsilon_{\gamma,\mathrm{MeV}}^{\mathrm{ob},-1}. \qquad (11)$$

The cutoff energy of muon neutrino spectrum due to the pion cooling can be obtained by setting $t_{\pi,\mathrm{syn}} = \tau_\pi$,

$$\epsilon_{\nu_\mu,\mathrm{c}}^{\mathrm{ob}} = \frac{3.3 \times 10^8}{(1+z)}L_{\gamma,52}^{-1/2}\Gamma_{2.5}^2 R_{14}\mathrm{GeV}. \qquad (12)$$

For antimuon neutrinos (and electron neutrinos) produced via the decay of muons, an extra break is caused by the muon cooling, which is

$$\epsilon_{\lambda,\mathrm{c}}^{\mathrm{ob}} = \frac{2.4 \times 10^7}{(1+z)}L_{\gamma,52}^{-1/2}\Gamma_{2.5}^2 R_{14}\mathrm{GeV}, \qquad (13)$$

where the subscript λ represents antimuon neutrino $\bar{\nu}_\mu$ or electron neutrino ν_e.

Assuming that the fraction of the amount of charged pions is $\Re = 1/2$, from equations (3) and (9), we get the spectrum of muon neutrinos produced by the pion decay,

$$(\epsilon_{\nu_\mu}^{\mathrm{ob}})^2 \frac{dn_{\nu_\mu}}{d\epsilon_{\nu_\mu}^{\mathrm{ob}}}$$

$$= \frac{0.014}{y_1}\left(\frac{2}{\alpha+1}\right)\left(\frac{1}{1+z}\right)\frac{\eta_p F_\gamma^{\mathrm{ob}}}{\ln(\frac{\epsilon_{p,\max}^{\mathrm{ob}}}{\epsilon_{p,\min}^{\mathrm{ob}}})}\frac{L_{\gamma,52}}{\epsilon_{\gamma b,\mathrm{MeV}}^{\mathrm{ob}}\Gamma_{2.5}^2 R_{14}}$$

$$\times \begin{cases} \left(\frac{\epsilon_{\nu_\mu}^{\mathrm{ob}}}{\epsilon_{\nu,b}^{\mathrm{ob}}}\right)^{\beta-1}, & \epsilon_{\nu_\mu}^{\mathrm{ob}} \leq \epsilon_{\nu,b}^{\mathrm{ob}} \\ \left(\frac{\epsilon_{\nu_\mu}^{\mathrm{ob}}}{\epsilon_{\nu,b}^{\mathrm{ob}}}\right)^{\alpha-1}, & \epsilon_{\nu,b}^{\mathrm{ob}} < \epsilon_{\nu_\mu}^{\mathrm{ob}} \leq \epsilon_{\nu_\mu,\mathrm{c}}^{\mathrm{ob}} \\ \left(\frac{\epsilon_{\nu_\mu}^{\mathrm{ob}}}{\epsilon_{\nu,b}^{\mathrm{ob}}}\right)^{\alpha-1}\left(\frac{\epsilon_{\nu_\mu}^{\mathrm{ob}}}{\epsilon_{\nu_\mu,\mathrm{c}}^{\mathrm{ob}}}\right)^{-2}. & \epsilon_{\nu_\mu}^{\mathrm{ob}} > \epsilon_{\nu_\mu,\mathrm{c}}^{\mathrm{ob}} \end{cases} \qquad (14)$$

---

[5] In some other papers, $\epsilon_{p,\min}^{\mathrm{ob}} \simeq 4\Gamma m_p c^2$ or $\epsilon_{p,\min}^{\mathrm{ob}} \simeq 10\Gamma m_p c^2$ are adopted, since the relative Lorentz factor is order of 1-10, where higher values favor efficiency internal shocks.

[6] Hereafter, for brevity, we abandoned the coefficient k_1 and k_ℓ in the following equations, since $k_1 \simeq 1$ and $k_\ell \simeq 0$ approximately, where $k_\ell = \frac{\alpha-\beta}{\beta+1}\left(\frac{\epsilon_\ell^{\mathrm{ob}}}{\epsilon_{\ell,b}^{\mathrm{ob}}}\right)^{-2}$ with ℓ represents three flavors of neutrinos, i.e., electron neutrinos and muon(antimuon) neutrinos. But we still adopt that in our analytic calculations.

Similarly, the spectrum of antimuon (and electron) neutrinos produced by muon decay is approximated by

$$
(\epsilon_\lambda^{\rm ob})^2 \frac{dn_\lambda}{d\epsilon_\lambda^{\rm ob}}
$$

$$
= \frac{0.014}{y_1} \left(\frac{2}{\alpha+1} \right) \left(\frac{1}{1+z} \right) \frac{\eta_p F_\gamma^{\rm ob}}{\ln(\frac{\epsilon_{\rm p,max}^{\rm ob}}{\epsilon_{\rm p,min}^{\rm ob}})} \frac{L_{\gamma 52}}{\epsilon_{\gamma b,{\rm MeV}}^{\rm ob} \Gamma_{2.5}^2 R_{14}}
$$

$$
\times \begin{cases}
\left(\frac{\epsilon_\lambda^{\rm ob}}{\epsilon_{\nu,b}^{\rm ob}} \right)^{\beta-1}, & \epsilon_\lambda^{\rm ob} \le \epsilon_{\nu,b}^{\rm ob} \\
\left(\frac{\epsilon_\lambda^{\rm ob}}{\epsilon_{\nu,b}^{\rm ob}} \right)^{\alpha-1}, & \epsilon_{\nu,b}^{\rm ob} < \epsilon_\lambda^{ob} \le \epsilon_{\lambda,c}^{\rm ob} \\
\left(\frac{\epsilon_\lambda^{\rm ob}}{\epsilon_{\nu,b}^{\rm ob}} \right)^{\alpha-1} \left(\frac{\epsilon_\lambda^{ob}}{\epsilon_{\lambda,c}^{ob}} \right)^{-2}, & \epsilon_{\lambda,c}^{\rm ob} < \epsilon_\lambda^{\rm ob} < \epsilon_{\nu_\mu,c}^{\rm ob} \\
\left(\frac{\epsilon_\lambda^{\rm ob}}{\epsilon_{\nu,b}^{\rm ob}} \right)^{\alpha-1} \left(\frac{\epsilon_\lambda^{ob}}{\epsilon_{\lambda,c}^{ob}} \right)^{-2} \left(\frac{\epsilon_\lambda^{ob}}{\epsilon_{\nu_\mu,c}^{ob}} \right)^{-2}, & \epsilon_{\nu_\mu,c}^{\rm ob} < \epsilon_\lambda^{ob}
\end{cases}
\tag{15}
$$

.Then, one can obtain the $\nu_\mu + \bar{\nu}_\mu$ spectrum after considering the neutrino oscillation effect by substituting equations (14) and (15) into equation (4).

2.1.2. Neutrino spectrum in the internal shock scenario

In this subsection, we assume the standard internal shock scenario with the dissipation radius at $R = 2\Gamma^2 c t_{\rm v}^{\rm ob}/(1+z)$, where $t_{\rm v}^{\rm ob}$ is the observed variability timescale of GRB emission. The conversion fraction $f_{p\gamma}$ is given by

$$
f_{p\gamma}(\epsilon_{\rm p}^{\rm ob}) \simeq \frac{0.18}{y_1} \left(\frac{2}{\alpha+1} \right) \frac{L_{\gamma 52}}{\epsilon_{\gamma b,{\rm MeV}}^{\rm ob} \Gamma_{2.5}^4 t_{\rm v,-2}^{\rm ob}}
$$

$$
\times \begin{cases}
\left(\frac{\epsilon_p^{\rm ob}}{\epsilon_{\rm p,b}^{\rm ob}} \right)^{\beta-1}, & \epsilon_p \le \epsilon_{\rm p,b}^{\rm ob} \\
\left(\frac{\epsilon_p^{\rm ob}}{\epsilon_{\rm p,b}^{\rm ob}} \right)^{\alpha-1}. & \epsilon_p > \epsilon_{\rm p,b}^{\rm ob}
\end{cases}
\tag{16}
$$

Then the spectrum of muon neutrinos produced via pion decay is approximated by

$$
(\epsilon_{\nu_\mu}^{\rm ob})^2 \frac{dn_{\nu_\mu}}{d\epsilon_{\nu_\mu}^{\rm ob}} = \frac{0.023}{y_1} \left(\frac{2}{\alpha+1} \right) \frac{\eta_p F_\gamma^{\rm ob}}{\ln(\frac{\epsilon_{\rm p,max}^{\rm ob}}{\epsilon_{\rm p,min}^{\rm ob}})} \frac{L_{\gamma,52}}{\epsilon_{\gamma b,{\rm MeV}}^{\rm ob} \Gamma_{2.5}^4 t_{\rm v,-2}^{\rm ob}}
$$

$$
\times \begin{cases}
\left(\frac{\epsilon_{\nu_\mu}^{\rm ob}}{\epsilon_{\nu,b}^{\rm ob}} \right)^{\beta-1}, & \epsilon_{\nu_\mu}^{\rm ob} \le \epsilon_{\nu,b}^{\rm ob} \\
\left(\frac{\epsilon_{\nu_\mu}^{\rm ob}}{\epsilon_{\nu,b}^{\rm ob}} \right)^{\alpha-1}, & \epsilon_{\nu,b}^{\rm ob} < \epsilon_{\nu_\mu}^{\rm ob} \le \epsilon_{\nu_\mu,c}^{\rm ob} \\
\left(\frac{\epsilon_{\nu_\mu}^{\rm ob}}{\epsilon_{\nu,b}^{\rm ob}} \right)^{\alpha-1} \left(\frac{\epsilon_{\nu_\mu}^{\rm ob}}{\epsilon_{\nu_\mu,c}^{\rm ob}} \right)^{-2}, & \epsilon_{\nu_\mu}^{\rm ob} > \epsilon_{\nu_\mu,c}^{\rm ob}
\end{cases}
\tag{17}
$$

and the spectrum of antimuon(electron) neutrinos produced via muon decay is approximated by

$$
(\epsilon_\lambda^{\rm ob})^2 \frac{dn_\lambda}{d\epsilon_\lambda^{\rm ob}} = \frac{0.023}{y_1} \left(\frac{2}{\alpha+1} \right) \frac{\eta_p F_\gamma^{\rm ob}}{\ln(\frac{\epsilon_{\rm p,max}^{\rm ob}}{\epsilon_{\rm p,min}^{\rm ob}})} \frac{L_{\gamma,52}}{\epsilon_{\gamma b,{\rm MeV}}^{\rm ob} \Gamma_{2.5}^4 t_{\rm v,-2}^{\rm ob}}
$$

$$
\times \begin{cases}
\left(\frac{\epsilon_\lambda^{\rm ob}}{\epsilon_{\nu,b}^{\rm ob}} \right)^{\beta-1}, & \epsilon_\lambda^{\rm ob} \le \epsilon_{\nu,b}^{\rm ob} \\
\left(\frac{\epsilon_\lambda^{\rm ob}}{\epsilon_{\nu,b}^{\rm ob}} \right)^{\alpha-1}, & \epsilon_{\nu,b}^{\rm ob} < \epsilon_\lambda^{\rm ob} \le \epsilon_{\lambda,c}^{\rm ob} \\
\left(\frac{\epsilon_\lambda^{\rm ob}}{\epsilon_{\nu,b}^{\rm ob}} \right)^{\alpha-1} \left(\frac{\epsilon_\lambda^{\rm ob}}{\epsilon_{\lambda,c}^{\rm ob}} \right)^{-2}, & \epsilon_{\lambda,c}^{\rm ob} < \epsilon_\lambda^{\rm ob} < \epsilon_{\nu_\mu,c}^{\rm ob} \\
\left(\frac{\epsilon_\lambda^{\rm ob}}{\epsilon_{\nu,b}^{\rm ob}} \right)^{\alpha-1} \left(\frac{\epsilon_\lambda^{\rm ob}}{\epsilon_{\lambda,c}^{\rm ob}} \right)^{-2} \left(\frac{\epsilon_\lambda^{\rm ob}}{\epsilon_{\nu_\mu,c}^{\rm ob}} \right)^{-2}, & \epsilon_{\nu_\mu,c}^{\rm ob} < \epsilon_\lambda^{\rm ob}
\end{cases}
\tag{18}
$$

where the cutoff energies are

$$
\epsilon_{\nu_\mu,c}^{\rm ob} = \frac{2.0 \times 10^8}{(1+z)^2} L_{\gamma,52}^{-1/2} \Gamma_{2.5}^4 t_{\rm v,-2}^{\rm ob} {\rm GeV}, \tag{19}
$$

and

$$
\epsilon_{\lambda,c}^{\rm ob} = \frac{1.4 \times 10^7}{(1+z)^2} L_{\gamma,52}^{-1/2} \Gamma_{2.5}^4 t_{\rm v,-2}^{\rm ob} {\rm GeV}, \tag{20}
$$

with λ representing antimuon and electron neutrinos ($\bar{\nu}_\mu$ and ν_e) produced by muon decay, and

$$
\frac{\epsilon_{\rm p,max}^{\rm ob}}{\epsilon_{\rm p,min}^{\rm ob}} = 1.0 \times 10^9 \Gamma_{2.5}^{3/2} (t_{\rm v,-2}^{\rm ob})^{1/2} L_{\gamma,52}^{-1/4} \epsilon_e^{1/4} \epsilon_B^{-1/4} g_1^{-1/2}. \tag{21}
$$

Substituting equations (17) and (18) into equation (4), we can obtain the neutrino spectrum analytically. To illustrate the difference between our calculation and the ICC calculation, we calculate the neutrino spectrum for one typical GRB with benchmark parameters, shown in Figure 1. Compared with the ICC calculation (the dark gray solid line), our spectrum (the purple solid line) consists of more structures resulting from the sum of the contributions by three flavors of neutrinos, for which both pion cooling, muon cooling and the oscillation effect are considered. Furthermore, the flux level predicted by our modified analytical calculation is a factor of ~ 20 lower than that obtained by ICC (Abbasi et al., 2011). This mainly arises from two differences in the calculation:

(I) We use equation (3), where the conversion fraction $f_{p\gamma}$ is a function of the proton energy ϵ_p as shown by equation (16), to normalize the neutrino flux to the proton flux, which means that only a fraction of protons can produce neutrinos efficiently. This corrects ICC's inaccurate use of energy-independent conversion fraction in the normalization of the neutrino flux (Li 2011; Hümmer et al. 2011; Murase et al. 2012). The calculation of Guetta et al. (2004) [7] normalized the flux based on the

---

[7] Guetta et al. (2004) calculated the neutrino spectrum by assuming a flat high-energy electron spectrum (i.e. $dN_e/d\gamma_e \propto \gamma_e^{-2}$) and using an electron equipartition fraction ϵ_e^G that represents the ratio of the nonthermal electron energy over one energy decade to the UHECR energy over one energy decade, and the neutrino flux is normalized by $\epsilon_\nu^2 dN_\nu/d\epsilon_\nu = (1/8)(1/\epsilon_e^G)(F_\gamma^{ob}/\ln 10)f_\pi$ (see their Eq. A19). Note that other normalization procedures are also possible, and this ϵ_e^G is typically larger than the conventional ϵ_e that is defined as the ratio of the total nonthermal electron energy to the total internal energy (including both thermal and nonthermal protons).

differential spectrum so that it does not suffer from this problem. The spectrum obtained with the calculation of Guetta et al. (2004)[8] is shown by the blue solid line in Figure 1, where the middle of equation (A.15) in their paper is used assuming the bolometric luminosity as the luminosity at the break energy. The flux is lower than the ICC result (the dark gray solid line in Figure 1) by a factor of ~ 4.

(II) In calculating the photon number density, we consider the photon energy distribution according to the real photon spectrum, reflected by the normalized coefficient $A_\gamma \simeq \frac{U_\gamma}{y_1 \epsilon_{\gamma b}^2}$, where y_1 is shown in equation (7), while ICC approximate the energy of all photons by the break energy of the photon spectrum. This leads to a flux a factor of $\sim$3-6 lower than the ICC result for typical α and β values and $\epsilon_{\gamma b} \sim 100 - 1000 \text{keV}$ in the GRB spectrum.

Finally, we get a neutrino spectral flux (purple solid line) lower than the one predicted by ICC (dark gray solid line) by a factor of ~ 20 for a typical GRB, as shown in Figure 1. Of course, the suppression factor is different for GRBs with different parameters.

2.2. Numerical Results

Besides the baryon resonance, the direct pion process, multi-pion process and the diffractive scattering also contribute to the total $p\gamma$ cross section. Therefore, in our numerical calculation, we adopt a more precise cross section for photomeson interaction, including three main channels, i.e., the Δ resonance process, direct pion process and multi-pion process. For simplicity, we assume that the inelasticity is $\xi = 0.2$ for $\bar{\epsilon}_\gamma < 983 \text{MeV}$ and $\xi = 0.6$ for $\bar{\epsilon}_\gamma \gtrsim 983 \text{MeV}$(Atoyan & Dermer 2001). Then, inserting the cross sections and inelasticity into equation (1) and using equation (2), we can get the fractions of protons energy converted to pions. The average fractions of the charged pions are set to $\Re_\Delta = 1/3$ for Δ Resonance process, $\Re_{\text{dir}} = 2/3$ for direct pion production, and $\Re_{\text{mul}} = 2/3$ for multipion production, based on numerical investigations (Mucke et al. 1999, 2000, Murase & Nagataki 2006a, b, Murase et al., 2006, Murase, 2007, Baerwald et al. 2011). In addition, we assume the neutrino energy is $\epsilon_\nu = 0.05\epsilon_p$ for Δ-resonance and direct pion production channels, and $\epsilon_\nu = 0.03\epsilon_p$ for multipion production channel. Inserting these quantities into equations (1), (2) and then (5), we can obtain the spectrum of neutrino emission produced via the three dominant channels. Although this simplified numerical approach

is different from more detailed, fully numerical calculations (Murase & Nagataki 2006a,b; Murase 2007; Baerward et al. 2011), it is enough for our purpose and saves calculation time.

In Figure 1, we also show this numerical result (the red solid line) for comparison. The flux obtained with this numerical calculation is about 2-3 times larger than the analytical result in the energy range 10^5GeV–3×10^6 GeV for typical GRB , consistent with Murase & Nagataki (2006a, b) and Baerwald et al. (2011). So the analytic calculation presented in the above section can still be used as a rough approximation.

2.3. Confronting the calculations with IC59+40 observations

215 GRBs are observed during the operations in the 40-string and 59-string configurations of IceCube, yielding negative results. In this section, we calculate the neutrino flux for the same 215 GRBs using the same burst parameters as ICC. The information for these samples was taken from the website grbweb.icecube.wisc.edu[9] and GCN. For the unmeasured parameters, we adopt the same average values as in Abbasi et al. (2010, 2011a). We assume a ratio of proton energy to radiation energy $\eta_p = 10$, equivalent to $1/f_e = 10$ in ICC calculation. We adopt the internal shock model with shock radius at $R = 2\Gamma^2 ct_v^{\text{ob}}/(1 + z)$, where the Lorentz factor is $\Gamma = 10^{2.5}$ and the observed variability timescale is $t_v^{\text{ob}} = 0.01 \text{s}$ for each long GRB and $t_v^{\text{ob}} = 0.001 \text{s}$ for each short GRB as the ICC did. The diffuse neutrino flux can be obtained by the total neutrino fluence for 215 individual GRBs timing a factor $7.83 \times 10^{-9} \text{sr}^{-1} \text{s}^{-1}$ with the assumption that a total of 667 uniformly GRBs are generated per year. By adopting the effective area of IC59 and IC40 as a function of zenith angle, we can calculate the expected number of neutrinos with energy from 10^5 GeV to 3×10^6 GeV (Abbasi et al. 2010, 2011a). The corresponding combined 90% confidence level (CL) upper limit spectrum can be obtained by assuming that the limit amount of neutrino events is $n_{\text{lim}} \simeq 1.9$ in the energy range from 10^5 GeV to 3×10^6 GeV as in the IceCube collaboration (2011).

In Figure 2, we show the 215 neutrino spectra (light red thin solid lines) for individual GRBs. The sum of them is presented as the red thick solid line, which is about a factor of ~ 10 lower than that predicted by ICC (the dark gray solid line; The IceCube collaboration 2011). As we can see, the neutrinos predicted by ICC2010 and GT2004 (dark gray solid line and blue solid line) are above the 90% CL upper limits (dark gray dashed line and blue dashed line) for the combined IC40 and IC59 data analysis, while our predicted neutrino flux is below the corresponding upper limit (the red dashed line). We find that the total expected number of neutrinos with energy from 10^5 GeV to 3×10^6 GeV is 0.74, which is 36% of the 90% CL upper limit.

3. CONSTRAINTS ON THE FIREBALL PROPERTIES

3.1. Uncertainty in the dissipation radius

In § 2.1.1, we do not assume a specific dissipation model for GRB emission, but leave the dissipation radius

---

[8] In our paper, we used the nonthermal baryon-loading parameter η_p, defined as the ratio between the total energy in accelerating protons and the total radiation energy at observed bands, to normalize the neutrino flux through $\epsilon_\nu^2 dN_\nu/d\epsilon_\nu = (1/8)(\eta_p/\ln(\epsilon_{p,\text{max}}/\epsilon_{p,\text{min}}))F_\gamma^{ob} f_{p\gamma}$. The lines of "modified Guetta et al. (2004) " in Figures 1 and 2 are obtained by using the benchmark value of $\eta_p = 10$, which corresponds to $\epsilon_e^G = \ln(\epsilon_{p,\text{max}}/\epsilon_{p,\text{min}})/\ln(10)(1/\eta_p) \sim 1$ in Eq.(A19) in Guetta et al. (2004). Choosing $\epsilon_e^G = 0.1$ in Guetta et al. (2004) would correspond to a higher baryon loading factor of $\eta_p = \ln(\epsilon_{p,\text{max}}/\epsilon_{p,\text{min}})/\ln(10)(1/\epsilon_e^G) \sim 100$ in our paper. Note that the GRB-UHECR hypothesis might suggest such high loading factors if the local GRB rate is $0.01 - 0.1 \text{Gpc}^{-3}\text{yr}^{-1}$ or the local luminosity density is significantly smaller than $\sim 10^{44}\text{ergMpc}^{-3}\text{yr}^{-1}$, and those relatively optimistic cases are constrained by IceCube under reasonable assumptions, as expected in Murase & Nagataki (2006b)."

[9] For some information from this website with typo, which is different from GCN, we take the information from GCN.

as a free parameter. Internal shocks happen over a wide parameter range (e.g. Nakar & Piran 2002), and even larger radii are suggested in some other dissipation models (e.g., Narayan & Kumar 2009, Zhang & Yan 2010). In Figure 3, we show the total neutrino spectra for 215 GRBs by assuming some fixed dissipation radii for every GRBs in the range $R = 10^{12}\text{cm} - 10^{16}\text{cm}$ [10]. It shows that the neutrino flux for the case of $R = 10^{12}\text{cm}$ (the black solid line) would exceed the corresponding IceCube upper limit (the black dashed line) as long as the baryon loading factor is sufficiently greater than unity. If we fix $\eta_p = 10$, the non-detection requires that the dissipation radius should be larger than $4 \times 10^{12}\text{cm}$. We note that, when the emission radius is too small, the maximum energy of accelerating particles is limited due to strong photohadronic and/or radiation cooling, and neutrino emission can be more complicated due to strong pion/muon cooling, so a more careful study is needed to obtain quantitative constrains on η_p in this regime. On the other hand, the larger dissipation radius leads to lower neutrino flux and higher cooling break energy according to equations (12) and (13). The shift of the first break to higher energies for larger dissipation radii is due to that those GRBs with $\alpha > 1$, whose neutrino spectral peaks locate at the cooling breaks, contribute dominantly to the neutrino flux.

3.2. *Uncertainty in the bulk Lorentz factor*

In the previous subsections, we took either the variability or dissipation radius as a principal parameter, given a Lorentz factor, i.e. $\Gamma = 10^{2.5}$. For those bursts without measured redshift, we took $L_\gamma = 10^{52}\text{erg s}^{-1}$ for the peak luminosity, as done by ICC. However, it was found recently that, the bulk Lorentz factor could vary significantly among bursts, and there is an inherent relation between the Lorentz factor and the isotropic energy or the peak luminosity (Liang et al. 2011; Ghirlanda et. al. 2011). As shown by Equations (17) and (18), the neutrino flux is very sensitive to the bulk Lorentz factor, so we can use the inherent relation to obtain more realistic values for the Lorentz factors and, hence, more reliable estimate of the neutrino flux.

By identifying the onset time of the forward shock from the optical afterglow observations, Liang et al. (2011) and Lv et al. (2011) obtain the bulk Lorentz factors for a sample of GRBs. They further found a correlation between the bulk Lorentz factor and the isotropic energy of the burst, given by[11]

$$\Gamma_L = 118 E_{\text{iso},52}^{0.26}. \tag{22}$$

Ghirlanda et. al. (2011) revisit this problem with a large sample and obtain a relation as

$$\Gamma_G = 29.8 E_{\text{iso},52}^{0.51}. \tag{23}$$

Compared with the benchmark model which assumes $\Gamma = 10^{2.5}$ for all bursts, the value of Γ obtained from

these relations is lower for bursts with the isotropic energy $E_{\text{iso}} \lesssim (4.4 - 9.4) \times 10^{53}\text{erg}$.

Ghirlanda et. al. (2011) also obtained the relation between the bulk Lorentz factor and peak luminosity, i.e.

$$\Gamma_{G_L} = 72.1 L_{\gamma,52}^{0.49}. \tag{24}$$

The value of Γ obtained from this relation is lower than $10^{2.5}$ for bursts with luminosity $L_p < 2.0 \times 10^{53}\text{ergs}^{-1}$.

Yonetoku et al. (2004) and Ghirlanda et al. (2011) found an inherent relation between the peak energy of photon spectrum and the peak luminosity. Therefore one can obtain the peak luminosity from the observed break energy of the photon spectrum $\epsilon_{\gamma,b}^{\text{ob}}$ and the redshift z by adopting the $\epsilon_{\gamma,b}^{\text{ob}} - L_\gamma$ relation, which is

$$L_{\gamma G,52} = 7.54 \left[\epsilon_{\gamma b,\text{MeV}}^{\text{ob}}(1+z)\right]^{1.75}, \tag{25}$$

derived by Ghirlanda et. al. (2011).

We use the above inherent relations to calculate both the Lorentz factor Γ and the peak luminosity L_γ, and then calculate the neutrino flux produced by the same 215 GRBs, which is shown in Figure 4. The main differences in the neutrino spectrum resulted from using different choices of the value of the bulk Lorentz factor can be summarized as:

(i) The peak energy of the neutrino spectrum shifts to lower energy for the models adopting the relations in Ghirlanda et al. (2011) and Lv et al. (2011). This is due to that for the majority in the 215 GRBs, the values of Γ derived with these inherent relations are lower than the benchmark value $10^{2.5}$, which leads to a lower peak energy in the neutrino spectrum according to equation (11). Also, the cutoff energy shifts to lower energies for these models according to equations (19) and (20).

(ii) The peak flux of the neutrino spectrum increases for the two models which adopt the inherent relations. This is due to that, a lower Lorentz factor leads to higher neutrino production efficiency in the internal shock model. The predicted neutrino flux for both models adopting $E_{\text{iso}} - \Gamma$ relations in Ghirlanda et al. (2011) and Lv et al. (2011) exceed the IceCube upper limit, which implies a baryon ratio $\eta_p \lesssim 10$ if $t_v^{\text{ob}} = 0.01\text{s}$ for long GRBs is correct.

In the left panel of Figure 4, we take the redshift $z = 2.15$ for those long GRBs without measured redshift, the amount of which is about 84% of the total amount of GRBs. For the benchmark model, the neutrino flux would not be affected significantly since it is independent of the redshift according to equations (17) and (18). However, the value of redshift can affect the flux of the neutrino spectrum for models adopting the inherent relations. For a fixed observed fluence of the $\gamma-$ray emission, a smaller redshift will lead to a smaller peak luminosity or isotropic energy. As a result, the Lorentz factor, derived from the inherent relations, will be lower, which leads to a higher neutrino production efficiency. As shown in the right panel of Figure 4, the flux for the two models adopting inherent relations increase if we take $z = 1$ for those long GRBs without measured redshifts.

In the above discussions, we have implicitly assumed the baryon ratio $\eta_p = 10$ for GRBs, in accordance with the notation $f_e = 0.1$ in Abbasi et al. (2010). This value

---

[10] We note that, if the radius is smaller than the photosphere radius, the neutrino emission produced by $p - p$ interactions becomes important (Wang & Dai 2009; Murase 2008), which is not considered here.

[11] We adopt only the center value for the relationships presented hereafter.

comes from the assumption that the radiation efficiency for GRBs is typically 0.1 and that most of the dissipated internal energy goes into the accelerated protons. However, the fraction of energy in protons, and hence the value of η_p, are not well-known. The null result of Ice-Cube observations allows us to put some constraints on this value. Define $\eta_{p,c}$ as the critic value, above which GRBs would be detected by the corresponding IceCube configurations. In Table 1, we list the corresponding value of $\eta_{p,c}$ for the combined IC40 and IC59 analysis. However, one should keep in mind that $\eta_{p,c}$ depends on the choice of $t_{\rm v}^{\rm ob}$, so it should be larger for larger values of $t_{\rm v}^{\rm ob}$.

4. DIFFUSE NEUTRINO EMISSION FROM GRBS

Recently, IceCube also reported observations of diffuse neutrinos by the 40-string configuration. The non-detection yields an upper limit of 8.9×10^{-9}GeV cm^{-1}s^{-1}sr^{-1}, for the diffuse neutrino flux assuming an E^{-2} neutrino spectrum (Abbasi et al. 2011b). The expected diffuse GRB neutrino flux can be obtained by summing the contributions of all GRBs in the whole universe. To this aim, we also take into account the number distribution of GRBs over the luminosity (i.e., the luminosity function) as well as the number distribution at different redshifts. Although it is not relevant if the GRB parameters (Γ and R) do not depend on the luminosity, it affects results when one adopts specific relations such as equations (22) or (23) or (25).

We employ three different luminosity functions and the corresponding source density evolution functions to describe the distribution of the GRB number over luminosity and redshift. One luminosity function is suggested by Liang et al. (2007, hereafter LF-L),

$$\frac{dN}{dL_\gamma} = \rho_0 \Phi_0 \left[\left(\frac{L_\gamma}{L_{\gamma b}} \right)^{\alpha_1} + \left(\frac{L_\gamma}{L_{\gamma b}} \right)^{\alpha_2} \right]^{-1}, \qquad (26)$$

where $\rho_0 = 1.2$Gpc^{-3}yr^{-1} is the local event rate of GRBs, and Φ_0 is a normalization constant to assure the integral over the luminosity function being equal to the local event rate ρ_0. This luminosity function breaks at $L_{\gamma b} = 2.25 \times 10^{52}$erg s^{-1}, with indices $\alpha_1 = 0.65$ and $\alpha_2 = 2.3$ for each segment. The normalized number distribution of GRBs with redshift used by Liang et al. (2007) in obtaining this luminosity function is (Porciani & Madau 2001)

$$S(z) = 23 \frac{e^{3.4z}}{e^{3.4z} + 22.0}. \qquad (27)$$

Wanderman & Piran (2009) also suggested a luminosity function in the form of a broken power–law (hereafter LF-W)

$$\frac{dN}{dL_\gamma} = \rho_0 \Phi_0 \begin{cases} (\frac{L_\gamma}{L_{\gamma b}})^{-\alpha_1} & L < L_{\gamma b}, \\ (\frac{L_\gamma}{L_{\gamma b}})^{-\alpha_2} & L \geq L_{\gamma b}, \end{cases} \qquad (28)$$

where $\rho_0 = 1.3$Gpc^{-3}yr^{-1}, $\alpha_1 = 1.2$, $\alpha_2 = 2.4$ and break luminosity $L_{\gamma b} = 10^{52.5}$erg s^{-1}. The corresponding normalized number distribution with redshift is described by

$$S(z) = \begin{cases} (1+z)^{2.1} & z < 3, \\ (1+z)^{-1.4} & z \geq 3. \end{cases} \qquad (29)$$

Another luminosity function we consider here is suggested by Guetta & Piran (2007, hereafter LF-G), which is in the same form as that of Wanderman & Piran (2009), but with different parameters, i.e., $\rho_0 = 0.27$Gpc^{-3}yr^{-1}, $\alpha_1 = -1.1$, $\alpha_2 = -3.0$ and $L_{\gamma b} = 2.3 \times 10^{51}$erg s^{-1}. It implies a smaller local event rate and fewer GRBs at the high luminosity end. This luminosity function is obtained based on the assumption that the rate of GRBs follows the star formation history given by Rowan-Robinson (1999), i.e.

$$S(z) = \begin{cases} 10^{0.75z} & z < 1, \\ 10^{0.75} & z \geq 1. \end{cases} \qquad (30)$$

Denoting the differential neutrino number generated by a GRB with luminosity L_γ at local redshift z by $dn_\nu/d\epsilon_\nu$, the injection rate of neutrinos per unit time per comoving volume then can be obtained by

$$\Psi(\epsilon_\nu) = \rho(z) \int \frac{dn_\nu}{d\epsilon_\nu}(L_\gamma, \epsilon_\nu) \frac{dN}{dL_\gamma}(L_\gamma) dL_\gamma, \qquad (31)$$

where $\rho(z) \equiv \rho_0 S(z)$ is the event rate density in the rest frame. Considering the cosmological time dilation and the particle number conservation, a neutrino with energy ϵ_ν observed at the Earth must be produced at redshift z with energy $(1+z)\epsilon_\nu$ and $\Psi_\nu(\epsilon_\nu^{\rm ob})d\epsilon_\nu^{\rm ob} = (1+z)\Psi_\nu[(1+z)\epsilon_\nu^{\rm ob}]d\epsilon_\nu^{\rm ob}$. The total observed diffuse neutrino flux can then be integrated over redshift,

$$\frac{dN_{\rm tot}}{d\epsilon_\nu^{\rm ob}} = \int_0^{z_{\max}} \frac{1}{4\pi} \Psi[(1+z)\epsilon_\nu^{\rm ob}] \frac{cdz'}{H(z')} \qquad (32)$$

where $H(z) = H_0/\sqrt{(1+z)^3 \Omega_M + \Omega_\Lambda}$ is the Hubble constant at redshift z. Here we set $L_{\gamma,\min} = 10^{50}$erg s^{-1}, $L_{\gamma,\max} = 10^{54}$erg s^{-1} and $z_{\max} = 8$.

The results of diffuse neutrino flux are shown in Figure 5. In this plot, we show the diffuse muon neutrino spectra for both the case in which the bulk Lorentz factor of the GRBs follows the inherent relation suggested by Ghirlanda et al. (2011) (solid lines), as described in Sec. 3, and the case in which a constant value of Lorentz factor ($\Gamma = 10^{2.5}$) is assumed for all GRBs (dashed lines). The photon spectrum of GRBs is assumed to be a broken power-law spectrum described by equation (6) with the $\alpha = 1$ and $\beta = 2$, and the break energy of photon spectrum is calculated from the peak luminosity of GRBs via the relationship shown in equation (25). One can see from this plot that using different luminosity functions and associated source density evolution functions leads to very different flux of diffuse neutrinos. The expected flux for the LF-L function slightly exceeds the IC40 upper limit, while for the luminosity functions of LF-W and LF-G, the predicted flux is undetectable even with one–year full operation of IceCube. Particularly, the LF-G function results in a very low flux. This is not only because that the local event rate for this luminosity function is much lower, but also because that much more GRBs locate at the low luminosity end, which contribute lower neutrino flux than more luminous ones. To require the diffuse neutrino flux not to exceed the IC40 upper limit, we have $\eta_p \lesssim 8$ for the luminosity function of LF-L. For results in cases where the GRB parameters do not depend on the luminosity, see Murase & Nagataki (2006a), Murase et al. (2006), and Gupta & Zhang (2007).

5. CONCLUSIONS & DISCUSSIONS

The non-detection by the increasingly sensitive detector IceCube has provided interesting implications for various theoretical predictions of neutrino emission from GRBs. The IceCube collaboration reported that the IceCube 40-string and 59-string configurations have reached the sensitivity below the theoretical expectation, which, if true, would challenge the view that GRBs could be the sources for UHECRs. However, as also shown by previous works, we show that the IceCube collaboration used an overestimated theoretical flux in comparison with the IceCube instrument limit. We therefore revisit the analytic calculation of the neutrino flux, considering the realistic photon energy distribution in calculating the number density of fireball photons (instead of using the bolometric luminosity as the luminosity at the break energy), and using the appropriate normalization for the proton flux to evaluate the neutrino flux.

Using the modified formulas, we calculate the expected neutrino flux from the 215 GRBs observed during the operations of IceCube 40 and 59 strings configurations, assuming the same benchmark parameters as that used by the IceCube collaboration. The flux is about 36% of the 90% CL upper limit, consistent with the non-detection of IceCube for the combined data analysis of IC40 and IC59.

The benchmark model assumes constant values for the bulk Lorentz factor, the observed variability time and the peak luminosity for every burst. Recently, it was suggested that there are correlations between the bulk Lorentz factor and the isotropic energy, and between peak luminosity and the break energy of photon spectrum. Using such inherent relations to derive the Lorentz factor and the peak luminosity, we re-calculate the neutrino flux and find that the flux adopting these relations exceed the 90% CL upper limit for the assumption of $t_v^{ob} = 0.01$s for every long burst. This constrains the baryon ratio to be $\eta_p \lesssim 10$, which, however, could be relaxed if the variability times for most GRBs could be larger.

We also calculate the cumulative diffuse flux from GRBs using three different luminosity functions existing in the literature. For the luminosity functions of Guetta & Piran (2007) and Wandermann & Piran (2009), the expected flux is below the IceCube upper limit for both the case that assumes $\Gamma = 10^{2.5}$ for every bursts and the case considering the inherent relation between Γ and the peak luminosity. However, for the luminosity function obtained in Liang et al. (2007), the expected flux exceeds the IceCube limit for both cases. The non-detection of diffuse neutrinos then constrains the baryon ratio to be $\eta_p \lesssim 8$ in this case.

GRBs have been proposed to be potential sources for UHECRs, besides active galactic nuclei (e.g. Biermann & Strittmatter 1987; Takahara 1990; Berezinsky et al. 2006) and hypernovae/supernovae with relativistic components (Wang et al. 2007; Liu & Wang 2012; Murase et al. 2008). Neutrino detection would provide evidence for cosmic ray protons in GRBs. On the other hand, the non-detection by current IceCube can not yet exclude this connection[12], as the required baryon ratio for GRBs to be the sources of UHECRs is $\eta_p \simeq 5 - 10$ (Liu et al. 2011) for local GRB rate of $R \simeq 1\mathrm{Gpc}^{-3}\mathrm{yr}^{-1}$ (Liang et al. 2007; Wanderman & Piran 2009). Future more sensitive observations by IceCube or other neutrino telescopes may put more tight constraints on the baryon ratio and would be able to judge the GRB-UHECR connection.

[12] The argument that the GRB-UHECR connection is challenged by the IceCube non-detection in Ahlers et al. (2011) is based on the assumption that cosmic ray protons are produced by β-decay of neutrons from pγ-interactions that escape from the magnetic field.

REFERENCES

Abbasi, R., Abdou, Y., Abu-Zayyad, T., et al. 2010, ApJ, 710, 346

Abbasi, R., Abdou, Y., Abu-Zayyad, T., et al. 2011a, Physical Review Letters, 106, 141101

Abbasi, R., Abdou, Y., Abu-Zayyad, T., et al. 2011b, Phys. Rev. D, 84, 082001

Ahlers, M., Gonzalez-Garcia, M. C., & Halzen, F. 2011, Astroparticle Physics, 35, 87

Atoyan, A., & Dermer, C. D. 2001, Physical Review Letters, 87, 221102

Baerwald, P., Hümmer, S., & Winter, W. 2011, Phys. Rev. D, 83, 067303

Berezinsky, V., Gazizov, A. Z. and Grigorieva S. I. , 2006, Phys. Rev. D 74, 043005.

Biermann, P. L., & Strittmatter, P. A. 1987, ApJ, 322, 643

Dai, Z. G., & Lu, T. 2001, ApJ, 551, 249

Dermer, C. D. 2002, ApJ, 574, 65

Dermer C. D., Atoyan A., 2006, New J. Phys., 8, 122

Ghirlanda, G., Nava, L., Ghisellini, G., et al. 2012, MNRAS, 420, 483

Giannios, D. 2010, MNRAS, 408, L46

Guetta, D., Hooper, D., Alvarez-Mun˜Iz, J., Halzen, F., & Reuveni, E. 2004, Astroparticle Physics, 20, 429

Guetta, D., & Piran, T. 2007, Journal of Cosmology and Astroparticle Physics, 7, 3

Gupta, N., & Zhang, B. 2007, Astroparticle Physics, 27, 386

Hümmer, S., Baerwald, P., & Winter, W. 2011, arXiv:1112.1076

The IceCube Collaboration 2011, arXiv:1111.2741

Takahara, F. 1990, Progress of Theoretical Physics, 83, 1071

Karle, A., & for the IceCube Collaboration 2010, arXiv:1003.5715

Kashti, T., & Waxman, E. 2005, Physical Review Letters, 95, 181101

Kumar, P., & Narayan, R. 2009, MNRAS, 395, 472

Li, Z. 2012, Phys. Rev. D, 85, 027301

Liang, E., Zhang, B., Virgili, F., & Dai, Z. G. 2007, ApJ, 662, 1111

Liang, E.-W., Yi, S.-X., Zhang, J., et al. 2010, ApJ, 725, 2209

Liu, R.-Y., Wang, X.-Y., & Dai, Z.-G. 2011, MNRAS, 418, 1382

Liu, R. Y. & Wang, X. Y., 2012, ApJ, 746, 40

Lv, J., Zou, Y.-C., Lei, W.-H., et al. 2011, arXiv:1109.3757

Mucke, A., Rachen, J. P., Engel, R., Protheroe, R. J., & Stanev, T. 1999, Publications of the Astronomical Society of Australia, 16, 160

Mücke, A., Engel, R., Rachen, J. P., Protheroe, R. J., & Stanev, T. 2000, Computer Physics Communications, 124, 290

Murase, K., & Nagataki, S. 2006a, Physical Review Letters, 97, 051101

Murase, K., & Nagataki, S. 2006b, Phys. Rev. D, 73, 063002

Murase, K., Ioka, K., Nagataki, S., & Nakamura, T. 2006, ApJ, 651, L5

Murase, K. 2007, Phys. Rev. D, 76, 123001

Murase, K, 2008, Physical Review D, 78, 101302

Murase, K., Ioka, K., Nagataki, S., & Nakamura, T. 2008, Phys. Rev. D, 78, 023005

Murase, K., Asano, K., Terasawa, T., & Mészáros, P. 2012, ApJ, 746, 164

Nagataki, S., Kohri, K., Ando, S., & Sato, K. 2003, Astroparticle Physics, 18, 551

Narayan, R., & Kumar, P. 2009, MNRAS, 394, L117

Paczynski, B., & Xu, G. 1994, ApJ, 427, 708

Particle Data Group, Eidelman, S., Hayes, K. G., et al. 2004, Physics Letters B, 592, 1

Porciani, C., & Madau, P. 2001, ApJ, 548, 522

Rees, M. J., & Meszaros, P. 1994, ApJ, 430, L93

Rowan-Robinson, M. 1999, Ap&SS, 266, 291

Vietri, M. 1995, ApJ, 453, 883

Wanderman, D., & Piran, T. 2010, MNRAS, 406, 1944

Wang, X.-Y., Razzaque, S., Mészáros, P., & Dai, Z.-G. 2007, Phys. Rev. D, 76, 083009

Wang, X. Y. & Dai, Z. G., 2009, ApJ, 691, L67

Waxman, E. 1995, Physical Review Letters, 75, 386

Waxman, E., & Bahcall, J. 1997, Physical Review Letters, 78, 2292

Waxman, E., & Bahcall, J. N. 2000, ApJ, 541, 707

Yonetoku, D., Murakami, T., Nakamura, T., et al. 2004, ApJ, 609, 935
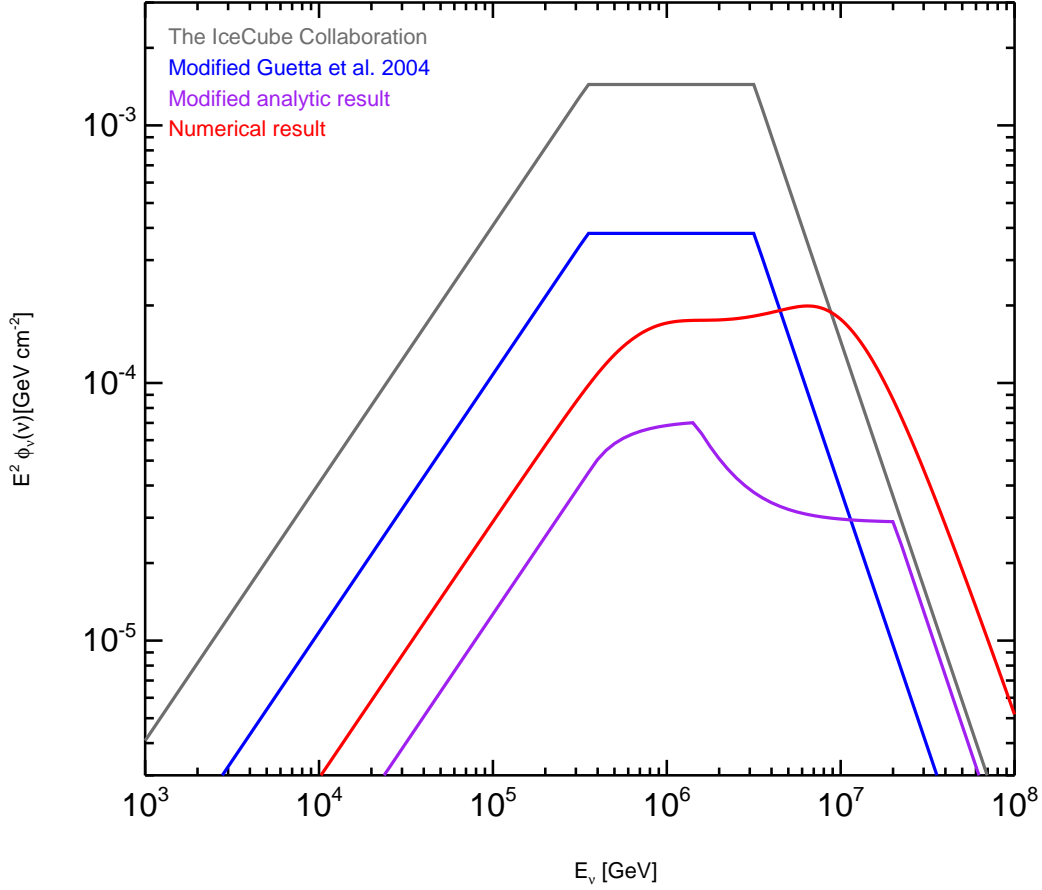
Zhang, B., & Yan, H. 2011, ApJ, 726, 90

FIG. 1.— The neutrino spectrum for one typical GRB obtained, respectively, with the method adopted by the IceCube collaboration (Abbasi et al, 2010, 2011a, the IceCube collaboration, 2011) (dark gray solid line), modified Guetta et al. (2004)'s method (blue solid line), our modified analytical method (purple solid line) and our numerical method (red solid line). The parameters used in the calculation for this GRB are: $\alpha = 1$, $\beta = 2$, fluence $F_\gamma^{\rm ob} = 10^{-5}{\rm erg\,cm^{-2}}$ (in 10keV to 1MeV), $z = 2.15$, peak energy $\epsilon_{\gamma,b}^{ob} = 200$keV, peak luminosity $L_\gamma = 10^{52}{\rm erg\,s^{-1}}$, bulk Lorentz factor $\Gamma = 10^{2.5}$, the observed variability timescale $t_{\rm v}^{\rm ob} = 0.01$s and the baryon ratio $\eta_p = 10$.

TABLE 1

$L_\gamma({\rm erg\,s^{-1}})$	Γ	z	$\eta_{p,c}$
10^{52}	$10^{2.5}$	2.15	26.0
		1	39.9
$L_{\gamma G}$	Γ_G	2.15	8.16
		1	7.79
$L_{\gamma G}$	Γ_L	2.15	9.07
		1	7.72

NOTE—The critical value of the baryon ratio $\eta_{p.c}$ for the combined IC40+IC59 analysis obtained by adopting different assumptions for the bulk Lorentz factor, peak luminosity and redshift (for long GRBs without measured redshifts). $L_{\gamma G}$ represents the peak luminosity obtained by using the $\epsilon_{\gamma b}^{\rm ob} - L_\gamma$ relation in Ghirlanda et al. (2011). Γ_G and Γ_L are the Lorentz factors obtained with the relations of $E_{\rm iso} - \Gamma$ in Lv et al. (2011) and Ghirlanda et al. (2011) respectively. Here, the observed variability timescale for long GRBs is assumed to be 0.01 s.
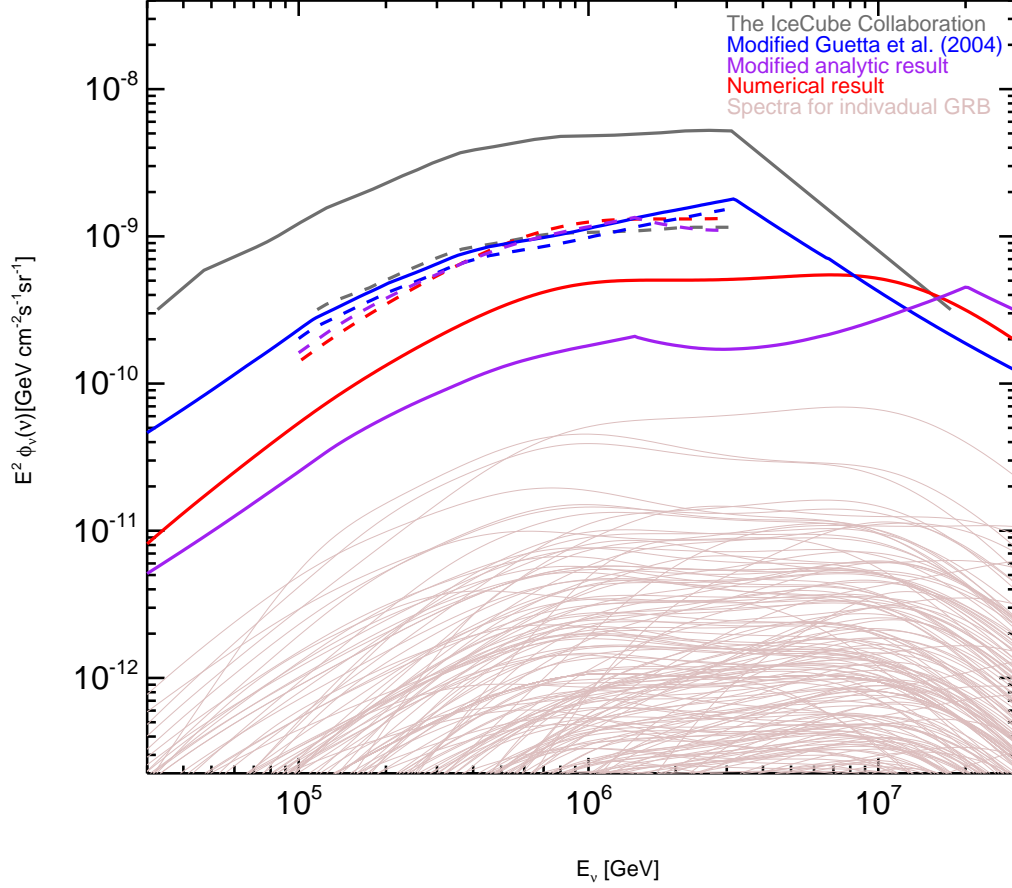
FIG. 2.— Neutrino spectra calculated numerically by adopting the internal shock radius $R = 2\Gamma^2 c t_\nu^{ob}/(1+z)$ for 215 GRBs (light red lines) observed during the operations in IceCube 40-string and 59-string configurations. We take the same GRB samples, the same assumptions for GRB parameters and the same effective area as function of zenith angle as those used by IceCube collaboration. The red thick solid line represents the sum of the 215 GRB neutrino spectra and the thick red dashed line is the corresponding 90% CL upper limit of IceCube. The thick dark gray solid line and dashed line are the predicted total neutrino spectrum and the corresponding 90 % CL upper limit given by the IceCube collaboration for the combined data analysis of IC40 and IC59 (The IceCube collaboration 2011). The blue solid and dashed lines correspond to the expected spectra and 90 % CL upper limit obtained by using the modified method in Guetta et al. (2004). The purple lines represent our modified analytical calculation as a comparison. For the above calculations, we adopt benchmark parameters, such as, the peak luminosity $L_\gamma = 10^{52}\,\mathrm{erg\,s^{-1}}$, the observed variability timescale $t_v^{ob} = 0.01$s for long GRBs, the Lorentz factor $\Gamma = 10^{2.5}$ and the baryon ratio $\eta_p = 10$ for every GRB.
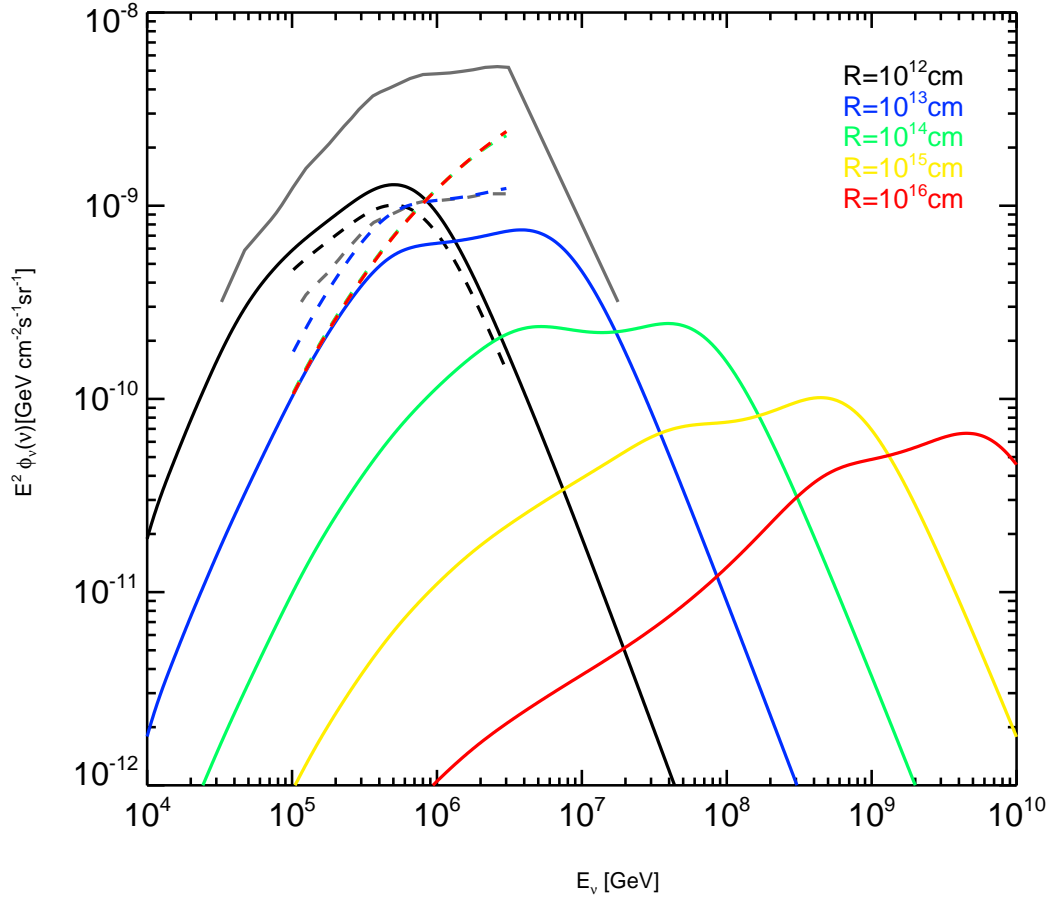
FIG. 3.— The spectra of the total neutrino emission produced by 215 GRBs assuming the same dissipation radius for every GRB at $R = 10^{12}$ cm (the black solid line), $R = 10^{13}$ cm (the blue solid line), $R = 10^{14}$ cm (the green solid line), $R = 10^{15}$ cm (the yellow solid line), $R = 10^{16}$ cm (the red solid line) respectively. The corresponding upper limits are shown by the dashed lines. Other parameters are the same as that used in Figure 2. Note here, the red, green and yellow dashed lines are overlapped with each other, because the spectrum shape of the red, green and yellow solid lines are similar in the energy range of $10^5 \, \mathrm{GeV} - 3 \times 10^6 \, \mathrm{GeV}$.
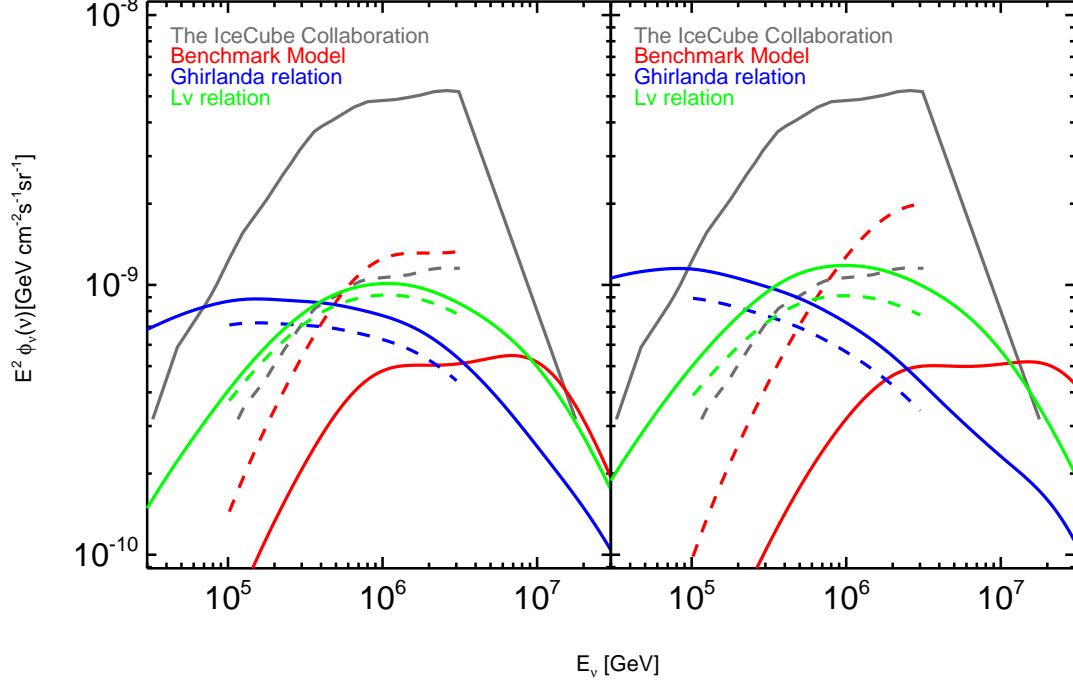
FIG. 4.— The spectra of the total neutrino emission produced by 215 GRBs assuming different fireball parameters in the standard internal shock model. The solid red line represents the spectrum that adopts benchmark parameters as in Figure 2. The solid blue line represents the spectrum that adopts the relations of $E_{\mathrm{iso}} - \Gamma$ and $\epsilon_{\gamma b}^{\mathrm{ob}} - L_\gamma$ in Ghirlanda et al. (2011). The solid green line represents the spectrum that adopts $E_{\mathrm{iso}} - \Gamma$ relation in Lv et al. (2011) and $\epsilon_{\gamma b}^{\mathrm{ob}} - L_\gamma$ relation in Ghirlanda et al. (2011). The dashed lines are the corresponding upper limit by IC40+IC59. Left panel: $z = 2.15$ is assumed for long GRBs without measured redshifts; Right panel: $z = 1$ is assumed for long GRBs without measured redshifts.
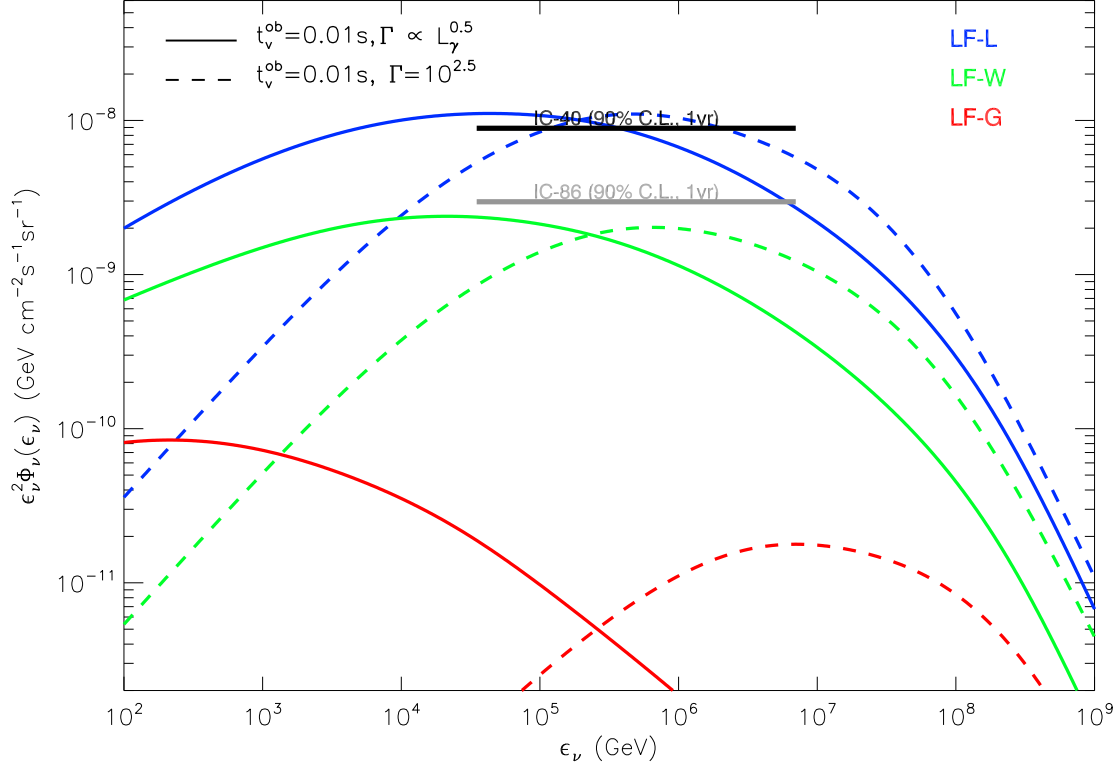
FIG. 5.— The expected diffuse muon neutrino flux from GRBs and the IceCube limits. The blue, green and red lines represent the fluxes obtained with luminosity functions of Liang et al. (2007), Wanderman & Piran (2009) and Guetta & Piran (2007) respectively. The solid line and dashed lines correspond to different assumptions about the Lorentz factor used in the calculation, but with the same observed variability timescale $t_v^{ob} = 0.01$ s for long GRBs and the same baryon loading ratio $\eta_p = 10$. The black thick solid line is the IC40 upper limit on the diffuse muon neutrino flux given in Abbasi et al. (2011b), while the dark gray solid line is the upper limit for one-year observation of the complete IceCube, extrapolated from the upper limit of IC40 via $A_{eff}^{IC86} \simeq 3A_{eff}^{IC40}$ (Karle 2011, Hümmer et al. 2011).